THE JOURNAL OF PHYSICAL CHEMISTRY Letters

pubs.acs.org/JPCL

Letter

Tuning the Carrier Lifetime in Black Phosphorene through Family Atom Doping

Hongli Guo, Weibin Chu, Qijing Zheng,* and Jin Zhao*

Cite This: *J. Phys. Chem. Lett.* 2020, 11, 4662−4667

Read Online

ACCESS | Metrics & More | Article Recommendations | Supporting Information

ABSTRACT: It is highly desirable to control the carrier lifetime in two-dimensional (2D) materials to suit the needs of various device functionalities. In this work, by *ab initio* nonadiabatic molecular dynamics simulation, we find the single atom doping from phosphorus family elements can sufficiently tune the carrier lifetime in black phosphorene (BP). Instead of forming electron−hole (e−h) recombination centers, the e−h recombination is suppressed by doping compared with the pristine BP. Moreover, it is found the carrier lifetime has a strong correlation with the mass of the doping atoms. A doping atom with larger mass leads to a longer lifetime. With the heaviest family element Bi doping, the carrier lifetime increases from 0.29 to 5.34 ns. This trend can be understood from the reduction of the nuclear velocity due to the heavy doping atom. We propose this conclusion can be extended to other monoelemental 2D semiconductors, which provides important guidance for the future design of functional nanodevices.

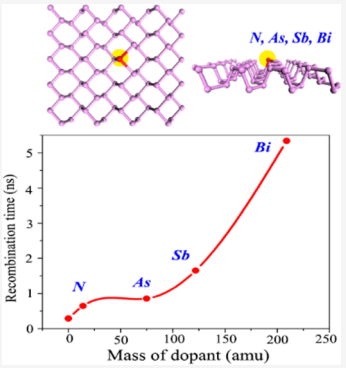

Downloaded via ZHEJIANG UNIV on April 8, 2026 at 06:50:50 (UTC).
See https://pubs.acs.org/sharingguidelines for options on how to legitimately share published articles.

Belonging to the newly developed two-dimensional (2D) materials, black phosphorus has attracted intense interest owing to its tunable thickness dependent direct band gap and high carrier mobility. Single layer black phosphorus is also known as black phosphorene (BP); it has a direct band gap of 1.5−2.0 eV, which enables the adsorption of visible sunlight. The carrier mobility is as high as 1000 $cm^2/(Vs)$, which guarantees its excellent performance in optoelectronic devices.[1−4]

The lifetime of the excited electron or hole, which is determined by the electron−hole (e−h) recombination, plays a crucial role at different strategies. For various applications in solar energy conversion and nanoscale optoelectronic devices, understanding and further customizing the carrier lifetime would make 2D BP highly adaptable to various application scenarios.[5−11] On one hand, several pump−probe ultrafast spectroscopy measurements of BP carrier dynamics[12−15] have been carried out and provided important information about the charge carrier dynamics and excited electron lifetimes. He et al. reported an excited state lifetime with a magnitude of 100 ps.[12] Mu and coauthors claimed that a fast electron−electron scattering in BP occurs at the 25 fs time scale and a slow electron decay occurs at a much longer time scale, 1.9 ps.[15] Suess et al. reported two time scales, 180 ps and 1.3 ns.[14] Ge et al. reported the whole decay process to be 1 ns.[13] One can see that different time scales have been obtained, suggesting that different sample quality (for example, the defect oxidization, thickness, and polymerization) and environment (e.g., the substrate and molecular adsorption) can affect the e−h recombination significantly. On the other hand, theoretical works by Long et al. and Zhang et al. have investigated how the different defects, oxidization, and H_2O adsorption affect the electron−hole recombination in BP.[16−18] They have shown that neither the defects nor the oxidization will form the e−h recombination centers. On the contrary, some of the defects can elongate the excited carrier lifetimes due to the monoelemental properties of 2D BP. Nevertheless, according to all these studies, how to control the e−h recombination dynamics is still not clear.

It is known that in the e−h recombination process the energy of excited carriers can convert to either photons (radiative process) or phonons (nonradiative process). The radiative e−h recombination is generally much slower than the nonradiative process.[19] Therefore, the lifetime of an excited carrier is mainly correlated with the nonradiative e−h recombination, which is determined by the electron−phonon (e−ph) interaction. In this manuscript, using *ab initio* nonadiabatic molecular dynamics (NAMD) simulation, we have investigated the e−h recombination dynamics in BP doped with a single atom of elements from the same family (N, As, Sb, Bi). Similar to defects in BP, for doped BP with family elements, no excess charges are induced, and thus e−h recombination centers are not formed. Instead, we find that family element doping can suppress the e−h recombination. Further, the excited carrier lifetime is found to be strongly

Received: April 28, 2020
Accepted: May 28, 2020
Published: May 28, 2020

ACS Publications

© 2020 American Chemical Society

https://dx.doi.org/10.1021/acs.jpclett.0c01300
J. Phys. Chem. Lett. 2020, 11, 4662−4667

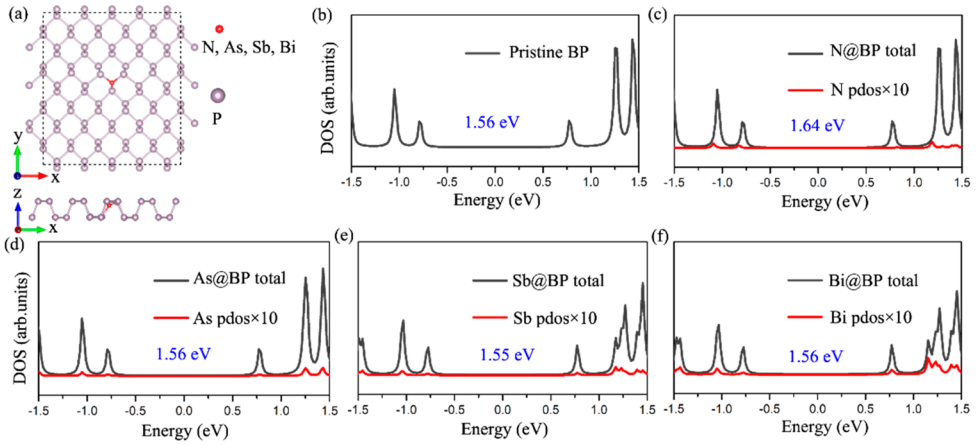

Figure 1. (a) Atomic structure of X (X = N, As, Sb, Bi) doped BP. (b–f) DOS of pristine BP and N, As, Sb, and Bi doped BP obtained by HSE functional; red lines denote the projected DOS of the dopant atoms.

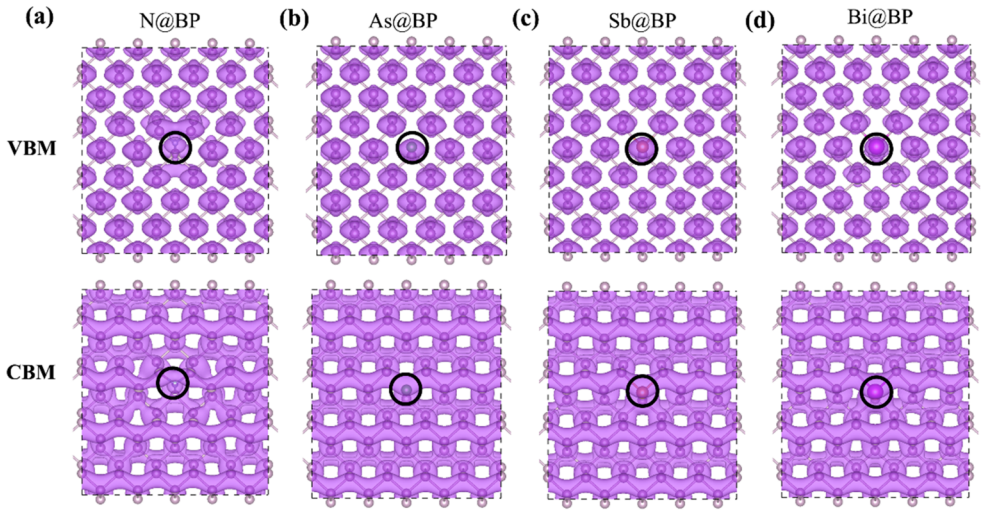

Figure 2. Orbital distributions of CBM and VBM for N, As, Sb, and Bi doped BP. The black circles indicate the positions of the dopants.

correlated with the mass of the doping element. A heavier doping atom induces a longer carrier lifetime. For Bi@BP, Bi has the largest mass among all the phosphorus family elements, the carrier lifetime is extended from 0.29 to 5.34 ns. Further analysis shows that the nonadiabatic coupling (NAC) element, which is the key factor determining the carrier lifetime, is proportional to the nuclear velocity in the molecular dynamics simulation. Therefore, the heavy doping atom can sufficiently reduce the nuclear velocity and thus suppress the e–h recombination notably. Our work suggests that doping with phosphorus family elements can sufficiently tune the carrier lifetime in BP, and we propose that this conclusion can be extended to other monoelemental 2D materials, providing valuable insights for the design of functional nanodevices based on 2D materials.

Our calculations employ the quantum-classical decoherence induced surface hopping (DISH) technique implemented within the time-dependent Kohn–Sham (TDKS) theory.[20,21] The geometry optimization, electronic structure, and adiabatic molecular dynamics trajectories are performed using Vienna Ab initio Simulation Package (VASP),[22] projector augmented wave (PAW)[23] method is used to describe electron–ion interaction, and Perdew–Burke–Ernzerhof (PBE) functional under the generalized gradient approximation (GGA)[24] is used to treat electron exchange–correction interactions. The nonadiabatic molecular dynamics simulations for e–h recombination are carried out with Hefei-NAMD code.[25] The phase-correction is applied using a similar method as that discussed in ref 26. We use a 5 × 4 × 1 supercell to model the BP monolayer. A 20 Å vacuum layer in the *z*-direction is used to eliminate spurious interactions between the periodic images. The relaxed lattice constants along the zigzag and armchair directions are a = 3.31 Å and b = 4.56 Å, respectively, for a unit cell of BP monolayer. For all the considered cases, we choose the kinetic energy cutoff of 400 eV and sample the first Brillouin zone at the Γ point only. All the structures are fully relaxed until the total energy and atomic forces are smaller than 10^{-6} eV and 0.01 eV/Å, respectively. After geometry optimization, the systems are heated to 300 K for 5 ps by velocity rescaling. Then, a 2 ps adiabatic molecular dynamics trajectory is obtained in the microcanonical ensemble with 1 fs time step. The simulation results are based on averaging 50 different initial configurations and 2000 trajectories sampled for each chosen initial structure. To simulate the charge carrier recombination dynamics on a nanosecond time scale, the 2 ps nonadiabatic Hamiltonians are iterated 500 times similarly to previous works.[16,17] It is known that the Perdew–Burke–Ernzerhof (PBE) functional underestimates the band gaps due

https://dx.doi.org/10.1021/acs.jpclett.0c01300
J. Phys. Chem. Lett. 2020, 11, 4662–4667

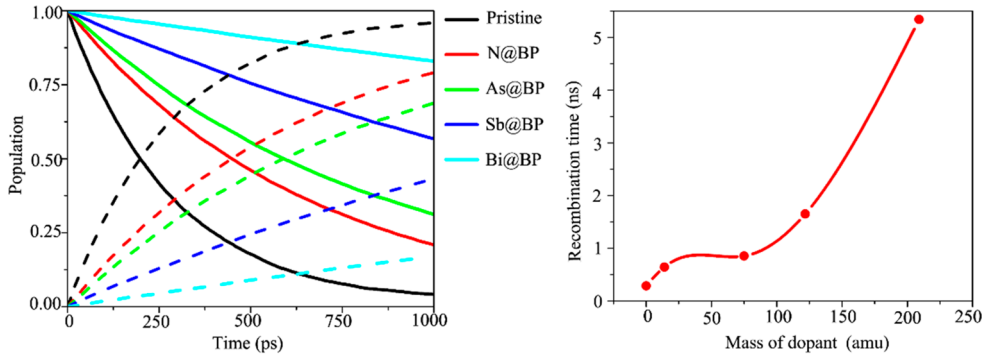

Figure 3. (a) The e−h recombination dynamics of pristine BP and N, As, Sb, and Bi doped BP at 300 K; solid lines are the dynamics of VBM, and dashed lines are those of CBM. (b) Recombination time as a function of the doping atom mass.

to its self-interaction error, so here we use the HSE06 functional to compute the electronic structure for all of the optimized geometries. In the TDKS Hamiltonian, the diagonal elements are the energies of Kohn−Sham (KS) orbitals. We scaled the PBE energies to the HSE06 values for these diagonal elements using the scissor operator and carried out the NAMD calculations. The comparison between the PBE and HSE results is shown in the Supporting Information.

Before we discuss the NAMD results, it is instructive to investigate the static electronic structures of doped BP. We have investigated five systems, including the pristine BP and doped BP with the P family elements N, As, Sb, and Bi. The geometric structure of doped BP and the density of states (DOS) of these five systems with the HSE funcitonal are shown in Figure 1. The band gap of pristine BP is 1.56 eV, which is almost the same for As@BP (1.56 eV), Sb@BP (1.55 eV), and Bi@BP (1.56 eV). The N@BP has a slightly larger band gap of 1.64 eV. For all the doped BP, the DOS suggest that the electronic orbitals of the impurity atoms are highly hybridized with the BP orbitals. There are no localized impurity states generated by the doping. Figure 2 shows the orbital distribution of conduction band minimum (CBM) and valence band maximum (VBM). It can be noticed that the doping atom only provides minor changes to the orbital distribution. The formation energy of the doping can be calculated as $E_{form} = E_{total} - (E_{Pv} + E_{dopant})$, where E_{total} is the energy of the doped BP, E_{Pv} is the energy of BP with a single P vacancy, and E_{dopant} is the energy of the doped atom. It suggests that family element doping is stable.

The nonradiative e−h recombination process starts after one electron is excited from the VBM to the CBM. The time-dependent excited hole populations on the VBM and CBM are shown in Figure 3. The e−h recombination time scales are fitted using exponential functions. It can be seen that none of these single atom dopings generates e−h recombination centers. On the contrary, all the dopings suppress e−h recombination. Further, the e−h recombination time scale has strong correlation with the doping atom mass. It increases along with the atomic mass. For BP doped with Bi, which has the largest mass, the e−h recombination time increases from 0.29 ns of the pristine BP to 5.34 ns.

In the nonradiative e−h recombination process, the carrier lifetime is dominantly affected by the e−ph coupling. In the *ab initio* NAMD simulation, as has been discussed in previous work, the carrier lifetime is determined by the NAC and phonon-induced coherence time (pure dephasing time), which are both strongly correlated with the phonon excitation and e−ph coupling.[26] Table 1 gives the NAC and the pure dephasing time of pristine and doped BP. The NAC is written as

Table 1. E_{form}, e−h Recombination Time, NAC, Dephasing Time, And Doping Atom Velocity of BP Doped with N, As, Sb, and Bi Single Atom[a]

	pristine BP	N@ BP	As@ BP	Sb@ BP	Bi@ BP
E_{form} (eV)		−1.08	−1.49	−1.31	−1.07
e−h recombination time (ns)	0.29	0.65	0.85	1.65	5.34
NAC (meV)	3.03	2.18	2.04	1.48	1.17
dephasing time (fs)	23.8	13.6	10.0	29.4	21.2
doping atom velocity (Å/ps)	4.7	6.8	4.3	2.8	1.6

[a]For pristine N, the averaged atom velocity is shown.

$$d_{jk} = \left\langle \varphi_j \left| \frac{\partial}{\partial t} \right| \varphi_k \right\rangle = \frac{\langle \varphi_j | \nabla_R H | \varphi_k \rangle}{\epsilon_k - \epsilon_j} \dot{R} \quad (1)$$

in which H is the Kohn−Sham Hamiltonian, φ_j, φ_k, ϵ_j, and ϵ_k are the corresponding wave functions and eigenvalues for electronic states j and k, and $\dot{R}$ is the velocity of the nuclei. One can see that the NAC is determined by three terms: e−ph coupling elements $\langle \varphi_j | \nabla_R H | \varphi_k \rangle$, the energy gap $\epsilon_k - \epsilon_j$, and the nuclear velocity $\dot{R}$. First, the $\langle \varphi_j | \nabla_R H | \varphi_k \rangle$ term can be understood from the CBM/VBM orbital distribution, the energy evolution of time-dependent KS states (shown in Figure 4), and their Fourier transform (FT) spectra (shown in Figure 5). The amplitude of energy fluctuation represents the e−ph coupling strength, and the FT spectra suggest the major phonon frequencies involved in it. Similar to that discussed in previous work, for the pristine BP, the CBM and VBM are mainly coupled with the out-of-plane A_g^1 mode and the in-plane B_{2g} and A_g^2 modes along the zigzag and armchair direction with frequencies around 400 cm^{-1}. VBM also couples with the out of plane acoustic phonon mode (ZA mode) below 100 cm^{-1}. As shown in Figures 4 and 5, the single atom doping with a family element does not change the e−ph properties significantly. It is consistent with the minor changes in the CBM and VBM orbital distributions shown in Figure 2.

Then we consider the energy gap term in NAC. As shown in Figures 1 and 4, only N@BP has a larger band gap than the pristine BP. All the other doping systems have similar band gap to the pristine BP. This partially explains why the N doping can suppress e−h recombination. The last term in NAC is the

https://dx.doi.org/10.1021/acs.jpclett.0c01300
J. Phys. Chem. Lett. 2020, 11, 4662−4667

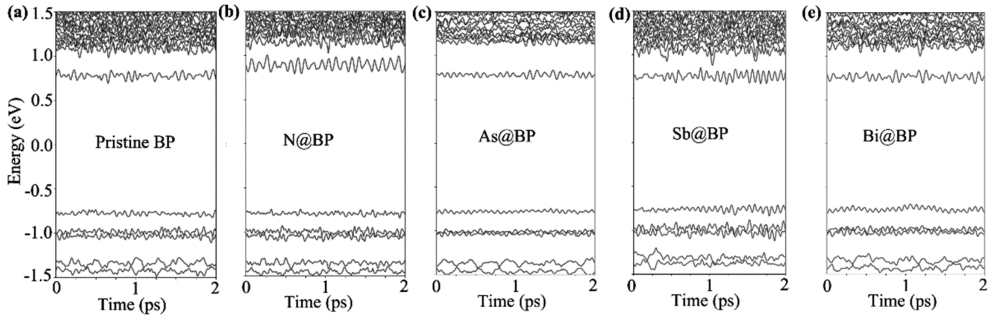

Figure 4. Energy evolution of KS states of pristine BP and N, As, Sb, and Bi doped BP at 300 K. The band gap is rescaled using the scissor operator by comparing the HSE results with the PBE results.

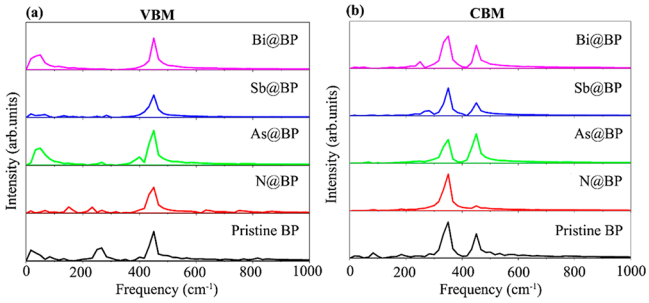

Figure 5. FT spectra of the time evolution of the VBM (a) and CBM (b) for pristine BP and N, As, Sb, and Bi doped BP at 300 K.

nuclear velocity. We have calculated the velocity of doped atoms in the molecular dynamics simulation, which are shown in Table 1. It clearly shows that the nuclear velocity decreases when the element mass increases, and it is roughly proportional to $\sqrt{m}$, where m represents the atomic mass. This trend is easy to understand since at the same temperature the kinetic energy of the doped atoms are appropriately the same. When the velocity of the doping atom is reduced by large mass, it also suppresses the movement of other P atoms nearby. Thus, the NAC decreases. The NAC dependence on the nuclear velocity successfully explains the correlation between the e−h recombination time and the element mass.

Besides the NAC, the pure dephasing time also plays a role in determining the e−h recombination time scale. It can be noted that the N@BP and As@BP systems have shorter dephasing times (13 and 10 fs), which can further suppress e−h recombination. Together with the larger band gap of N@BP comparing with pristine BP, it explains why N doping can suppress the e−h recombination, although N has a smaller mass compared with P.

Impurity doping and defects in semiconductors often introduce e−h recombination centers, which have been investigated in TiO_2 and MoS_2.[27−32] However, contrary to general expectation, our results show that single atom doping within the element family of P can suppress the e−h recombination in BP. Previous work showed that defects and small molecule adsorption on BP also suppress the nonradiative e−h recombination.[16−18] It was explained that the defects and adsorption can induce low-frequency phonon excitation, which will reduce both the NAC and dephasing time.[16,17] Moreover, here we reveal that the most important factor in the family element doping of BP is the element mass. Although the e−h recombination suppression in doping and defective BP are induced by different factors, in both cases, it is related to the monoelemental properties of BP. In this work, because BP is a monoelemental 2D material, doping with elements from the same family does not change the electronic structure and the electron−phonon coupling significantly.[33] The distinct impurity phonon shown in Cr−N doped TiO_2 is not found.[34] In this simple case, the element mass is the most distinct factor; it can reduce the nuclear velocity and then decrease the NAC. Thus, family element doping can be used to tune the e−h recombination rate in BP. Besides the family element doping, BP can also be doped by IVA or VIA elements. In these cases, the factor affecting the carrier lifetime may be more complex. Yet we propose the element mass is still an important factor. We propose this conclusion might be able to be extended to other monoelemental semiconductors, but future careful investigations are necessary to confirm this point.

It should be noted that in this work the e−h recombination process is simulated using a single-particle based NAMD simulation. For 2D materials like BP, we propose that the e−h interaction may play an important role in the excited carrier dynamics. However, when BP is used for practical applications, it is put on a substrate, and the Coulomb interaction is partially screened as discussed by Louie et al.[35] Yet, we still propose with the newly developed exciton dynamics simulation method, it is worth reinvestigating this problem again in the future. In addition, some interfacial phonon excitation may emerge to promote the e−h recombination in BP. And charge transfer would probably happen at the interface, which may separate the electron and hole in different layers and affect the recombination rate. Future work on the substrate effect, including screening effect, phonon excitation, and charge transfer process should be explored to address this problem.

To summarize, we have investigated the e−h recombination dynamics of doped BP with the family elements. We found that all the doped elements can suppress the e−h recombination. Moreover, the e−h recombination time scale is strongly correlated with the mass of the doping atom. Doping with Bi atom, which has the largest mass in the same family, can change the carrier lifetime from 0.29 to 5.34 ns. Analysis shows that the family element doping does not change the electronic structures and phonon frequencies significantly. Therefore, the mass of the element is the most crucial factor to affect the e−h recombination. The heavy doping atom can reduce the nuclear velocity and lower NAC, suppressing the e−h recombination. Our research suggests that doping with the family elements can tune the excited carrier lifetime effectively in BP. We propose that this conclusion may be able to be extended to other monoelemental semiconductors, and it provides valuable insights into functional device design based on 2D materials.

https://dx.doi.org/10.1021/acs.jpclett.0c01300
J. Phys. Chem. Lett. 2020, 11, 4662−4667

■ ASSOCIATED CONTENT

Supporting Information

The Supporting Information is available free of charge at https://pubs.acs.org/doi/10.1021/acs.jpclett.0c01300.

DOS obtained by PBE functional for the pristine and doped black phosphorene (PDF)

■ AUTHOR INFORMATION

Corresponding Authors

Qijing Zheng − *ICQD/Hefei National Laboratory for Physical Sciences at the Microscale, CAS Key Laboratory of Strongly-Coupled Quantum Matter Physics, and Department of Physics, University of Science and Technology of China, Hefei, Anhui 230026, China;* orcid.org/0000-0003-0022-3442; Email: zqj@ustc.edu.cn

Jin Zhao − *ICQD/Hefei National Laboratory for Physical Sciences at the Microscale, CAS Key Laboratory of Strongly-Coupled Quantum Matter Physics, and Department of Physics and CAS Center for Excellence in Quantum Information and Quantum Physics, University of Science and Technology of China, Hefei, Anhui 230026, China; Department of Physics and Astronomy, University of Pittsburgh, Pittsburgh, Pennsylvania 15260, United States;* orcid.org/0000-0003-1346-5280; Email: zhaojin@ustc.edu.cn

Authors

Hongli Guo − *ICQD/Hefei National Laboratory for Physical Sciences at the Microscale, CAS Key Laboratory of Strongly-Coupled Quantum Matter Physics, and Department of Physics, University of Science and Technology of China, Hefei, Anhui 230026, China; School of Physics and Technology, Center for Nanoscience and Nanotechnology, and Key Laboratory of Artificial Micro- and Nano-structures of Ministry of Education, Wuhan University, Wuhan 430072, China*

Weibin Chu − *ICQD/Hefei National Laboratory for Physical Sciences at the Microscale, CAS Key Laboratory of Strongly-Coupled Quantum Matter Physics, and Department of Physics, University of Science and Technology of China, Hefei, Anhui 230026, China; Department of Chemistry, University of Southern California, Los Angeles, California 90089, United States*

Complete contact information is available at: https://pubs.acs.org/10.1021/acs.jpclett.0c01300

Notes

The authors declare no competing financial interest.

■ ACKNOWLEDGMENTS

J.Z. acknowledges the support of the National Key Foundation of China, Department of Science and Technology, Grant Nos. 2017YFA0204904 and 2016YFA0200604, the National Natural Science Foundation of China (NSFC), Grant Nos. 11620101003, 11974322, and Anhui Initiative in Quantum Information Technologies (AHY090300). Q.Z. acknowledges the support of the National Natural Science Foundation of China (NSFC), Grant No. 11704363. H.G. acknowledges the funding from China Postdoctoral Science Foundation (Grant Nos. 2017M622498 and 2018T110789). Calculations were performed at Supercomputer Center of Wuhan University and the Environmental Molecular Sciences Laboratory at the PNNL, a user facility sponsored by the DOE Office of Biological and Environmental Research, and Supercomputing Center at USTC.

■ REFERENCES

(1) Long, G.; Maryenko, D.; Shen, J.; Xu, S.; Hou, J.; Wu, Z.; Wong, W. K.; Han, T.; Lin, J.; Cai, Y.; et al. Achieving ultrahigh carrier mobility in two-dimensional hole gas of black phosphorus. *Nano Lett.* **2016**, *16* (12), 7768−7773.

(2) Chen, X.; Wu, Y.; Wu, Z.; Han, Y.; Xu, S.; Wang, L.; Ye, W.; Han, T.; He, Y.; Cai, Y.; Wang, N. High-quality sandwiched black phosphorus heterostructure and its quantum oscillations. *Nat. Commun.* **2015**, *6* (1), 7315.

(3) Yang, S.; Zhang, K.; Ricciardulli, A. G.; Zhang, P.; Liao, Z.; Lohe, M. R.; Zschech, E.; Blom, P. W.; Pisula, W.; Müllen, K.; Feng, X. A delamination strategy for thinly layered defect-free high-mobility black phosphorus flakes. *Angew. Chem.* **2018**, *130* (17), 4767−4771.

(4) Qiao, J.; Kong, X.; Hu, Z.-X.; Yang, F.; Ji, W. High-mobility transport anisotropy and linear dichroism in few-layer black phosphorus. *Nat. Commun.* **2014**, *5* (1), 4475.

(5) Ni, J.; Li, L.; Lu, J. Phosphorus: an anode of choice for sodium-ion batteries. *ACS Ener. Lett.* **2018**, *3* (5), 1137−1144.

(6) Chowdhury, C.; Karmakar, S.; Datta, A. Capping black phosphorene by h-BN enhances performances in anodes for Li and Na ion batteries. *ACS Ener. Lett.* **2016**, *1* (1), 253−259.

(7) Du, Y.; Liu, H.; Deng, Y.; Ye, P. D. Device perspective for black phosphorus field-effect transistors: contact resistance, ambipolar behavior, and scaling. *ACS Nano* **2014**, *8* (10), 10035−10042.

(8) Wu, P.; Ameen, T.; Zhang, H.; Bendersky, L. A.; Ilatikhameneh, H.; Klimeck, G.; Rahman, R.; Davydov, A. V.; Appenzeller, J. Complementary black phosphorus tunneling field-effect transistors. *ACS Nano* **2019**, *13* (1), 377−385.

(9) Zhu, X.; Zhang, T.; Sun, Z.; Chen, H.; Guan, J.; Chen, X.; Ji, H.; Du, P.; Yang, S. Black phosphorus revisited: a missing metal-free elemental photocatalyst for visible light hydrogen evolution. *Adv. Mater.* **2017**, *29* (17), 1605776.

(10) Buscema, M.; Groenendijk, D. J.; Steele, G. A.; Van Der Zant, H. S.; Castellanos-Gomez, A. Photovoltaic effect in few-layer black phosphorus PN junctions defined by local electrostatic gating. *Nat. Commun.* **2014**, *5* (1), 4651.

(11) Niu, X.; Li, Y.; Zhang, Y.; Li, Q.; Zhou, Q.; Zhao, J.; Wang, J. Photo-oxidative degradation and protection mechanism of black phosphorus: insights from ultrafast dynamics. *J. Phys. Chem. Lett.* **2018**, *9* (17), 5034−5039.

(12) He, J.; He, D.; Wang, Y.; Cui, Q.; Bellus, M. Z.; Chiu, H.-Y.; Zhao, H. Exceptional and anisotropic transport properties of photocarriers in black phosphorus. *ACS Nano* **2015**, *9* (6), 6436−6442.

(13) Ge, S.; Li, C.; Zhang, Z.; Zhang, C.; Zhang, Y.; Qiu, J.; Wang, Q.; Liu, J.; Jia, S.; Feng, J.; Sun, D. Dynamical evolution of anisotropic response in black phosphorus under ultrafast photoexcitation. *Nano Lett.* **2015**, *15* (7), 4650−4656.

(14) Suess, R. J.; Jadidi, M. M.; Murphy, T. E.; Mittendorff, M. Carrier dynamics and transient photobleaching in thin layers of black phosphorus. *Appl. Phys. Lett.* **2015**, *107* (8), 081103.

(15) Mu, H.; Lin, S.; Wang, Z.; Xiao, S.; Li, P.; Chen, Y.; Zhang, H.; Bao, H.; Lau, S. P.; Pan, C.; et al. Black phosphorus-polymer composites for pulsed lasers. *Adv. Opt. Mater.* **2015**, *3* (10), 1447−1453.

(16) Zhang, L.; Chu, W.; Zheng, Q.; Benderskii, A. V.; Prezhdo, O. V.; Zhao, J. Suppression of Electron-Hole Recombination by Intrinsic Defects in 2D Monoelemental Material. *J. Phys. Chem. Lett.* **2019**, *10* (20), 6151−6158.

(17) Zhang, L.; Vasenko, A. S.; Zhao, J.; Prezhdo, O. V. Mono-elemental properties of 2D black phosphorus ensure extended charge carrier lifetimes under oxidation: time-domain ab initio analysis. *J. Phys. Chem. Lett.* **2019**, *10* (5), 1083−1091.

(18) Long, R.; Fang, W.; Akimov, A. V. Nonradiative electron-hole recombination rate is greatly reduced by defects in monolayer black

phosphorus: ab initio time domain study. *J. Phys. Chem. Lett.* **2016**, *7* (4), 653−659.
(19) Abakumov, V.; Perel, V. I.; Yassievich, I. *Nonradiative recombination in semiconductors*; Elsevier: 1991.
(20) Craig, C. F.; Duncan, W. R.; Prezhdo, O. V. Trajectory surface hopping in the time-dependent Kohn-Sham approach for electron-nuclear dynamics. *Phys. Rev. Lett.* **2005**, *95* (16), 163001.
(21) Tully, J. C. Molecular dynamics with electronic transitions. *J. Chem. Phys.* **1990**, *93* (2), 1061−1071.
(22) Kresse, G.; Furthmüller, J. Efficient iterative schemes forab initiototal-energy calculations using a plane-wave basis set. *Phys. Rev. B: Condens. Matter Mater. Phys.* **1996**, *54* (16), 11169−11186.
(23) Blöchl, P. E. Projector augmented-wave method. *Phys. Rev. B: Condens. Matter Mater. Phys.* **1994**, *50* (24), 17953−17979.
(24) Perdew, J. P.; Burke, K.; Ernzerhof, M. Generalized Gradient Approximation Made Simple. *Phys. Rev. Lett.* **1996**, *77* (18), 3865−3868.
(25) Zheng, Q.; Chu, W.; Zhao, C.; Zhang, L.; Guo, H.; Wang, Y.; Jiang, X.; Zhao, J. Ab initio nonadiabatic molecular dynamics investigations on the excited carriers in condensed matter systems. *Wiley Interdiscip. Rev.: Comput. Mol. Sci.* **2019**, *9* (6), No. e1411.
(26) Akimov, A. V.; Prezhdo, O. V. The PYXAID program for non-adiabatic molecular dynamics in condensed matter systems. *J. Chem. Theory Comput.* **2013**, *9* (11), 4959−4972.
(27) Martin, S. T.; Morrison, C. L.; Hoffmann, M. R. Photochemical mechanism of size-quantized vanadium-doped TiO_2 particles. *J. Phys. Chem.* **1994**, *98* (51), 13695−13704.
(28) Göpel, W.; Anderson, J.; Frankel, D.; Jaehnig, M.; Phillips, K.; Schäfer, J.; Rocker, G. Surface defects of TiO_2 (110): a combined XPS, XAES and ELS study. *Surf. Sci.* **1984**, *139* (2−3), 333−346.
(29) Cho, E.; Han, S.; Ahn, H.-S.; Lee, K.-R.; Kim, S. K.; Hwang, C. S. First-principles study of point defects in rutile TiO_{2-x}. *Phys. Rev. B: Condens. Matter Mater. Phys.* **2006**, *73* (19), 193202.
(30) KC, S.; Longo, R. C.; Addou, R.; Wallace, R. M.; Cho, K. Impact of intrinsic atomic defects on the electronic structure of MoS_2 monolayers. *Nanotechnology* **2014**, *25* (37), 375703.
(31) Liu, D.; Guo, Y.; Fang, L.; Robertson, J. Sulfur vacancies in monolayer MoS_2 and its electrical contacts. *Appl. Phys. Lett.* **2013**, *103* (18), 183113.
(32) Wang, H.; Zhang, C.; Rana, F. Ultrafast dynamics of defect-assisted electron-hole recombination in monolayer MoS_2. *Nano Lett.* **2015**, *15* (1), 339−345.
(33) Liu, Y.; Xu, F.; Zhang, Z.; Penev, E. S.; Yakobson, B. I. Two-dimensional mono-elemental semiconductor with electronically inactive defects: the case of phosphorus. *Nano Lett.* **2014**, *14* (12), 6782−6786.
(34) Zhang, L.; Zheng, Q.; Xie, Y.; Lan, Z.; Prezhdo, O. V.; Saidi, W. A.; Zhao, J. Delocalized impurity phonon induced electron-hole recombination in doped semiconductors. *Nano Lett.* **2018**, *18* (3), 1592−1599.
(35) Qiu, D. Y.; da Jornada, F. H.; Louie, S. G. Environmental screening effects in 2D materials: renormalization of the bandgap, electronic structure, and optical spectra of few-layer black phosphorus. *Nano Lett.* **2017**, *17* (8), 4706−4712.

https://dx.doi.org/10.1021/acs.jpclett.0c01300
J. Phys. Chem. Lett. 2020, 11, 4662−4667